On the role of covalent strain in protein function

Ryde, Ulf

Published in:
Recent research developments in protein engineering, Vol. 2

2002

Document Version:
Peer reviewed version (aka post-print)

On the role of covalent strain in protein function

Ulf Ryde

Department of Theoretical Chemistry
Lund University
Chemical Centre, P. O. Box 124
S–221 00 Lund, Sweden
Tel: 46–46–22245 02
Fax: 46–46–222 45 43
E-mail: Ulf.Ryde@teokem.lu.se

2001-02-21

Running title
Covalent strain in protein function

ABSTRACT

Strain has frequently been suggested to play an important role in the function of many proteins. Here, we review various definition of strain and discuss how it may be quantified. We show that covalent strain (i.e. strain caused by covalent interactions) plays a minor role for the function of all proteins we have studied, e.g. blue copper proteins, desulforedoxin, Cu_A in cytochrome *c* oxidase, and antibodies (the immunochromic effect). However, in small molecules, such as the haem group and macrocyclic model complexes, covalent strain may have a pronounced effect. In general, significant strain is seen when a molecule is constrained by covalent bonds in rings, whereas forces that determine the local environment in proteins, i.e. torsions and non-bonded interactions are too weak to distort a bound molecule or metal significantly.

INTRODUCTION

The suggestion that proteins use mechanical strain to gain catalytic power is an old hypothesis, discussed already by Pauling and Haldane [1, 2]. The most classical example of a protein for which strain has been suggested to play a functional role is lysozyme [3]. It was originally suggested that this protein forces its substrate to bind in an unfavourable conformation, similar to that of the transition state. However, theoretical calculations by Levitt and Warshel convincingly showed that strain has a negligible influence on the rate of this enzyme. Instead, the activation energy is reduced by favourable electrostatic interactions in the transition state [4]. This and other cases have led several leading biophysical chemists to argue strongly against strain as an important factor in enzyme catalysis and to conclude that a substrate molecule is normally more rigid than a protein [4–6]. However, we still see suggestions that strain should be important for the function of various enzymes [e.g. 7–9].

The two most well-known general hypotheses for protein strain are the entatic state [10,11] and the induced-rack theories [12,13]. Although most people consider these hypotheses to be similar [e.g. 15], Williams has strongly argued that this is not the case [11]. The induced-rack theory was presented by Malmström in 1964 [16]. It suggests that a protein can dictate the properties of a metal by presenting a preformed chelating site with very little flexibility, where the spatial arrangement of the ligands is in conflict with the geometrical

preference of the metal ion. Originally, it did not encompass entropic effects such as conformational changes or solvation effects [13]. It is based on the older rack mechanism formulated by Lumry and Eyring ten years earlier [14], according to which key functional groups can be distorted by the overall protein conformations, leading to anomalous properties.

The entatic state theory (from Greek "entasis", under tension or in a stretched state) was introduced by Vallee and Williams in 1968 [10], although some of the ideas had been presented earlier [11]. It suggests that some proteins contain a catalytically poised state intrinsic to the active site. In a recent review, the concept was further specified: An entatic state occurs in a protein when a group is forced into an unusual, energised, geometric or electronic state by misfitting to the protein fold [11].

In that review, Williams also discusses how the protein may energise or may be energised by a bound group in four different ways. In the first case, the protein is rigid and only the group distorts. This is called the entatic state. Alternatively, the group could be rigid and only the protein distorts, which is called the induced matrix state. The third alternative is that both the protein and the group are distorted. Williams distinguishes between a local (induced fit) or global distortion of the protein. The latter case is the rack state according to Williams. It should be noted, however, that Malmström considers the blue copper proteins (the typical example of the induced-rack theory) to be rigid and the metal distorted (i.e. entatic in Williams' nomenclature) [12,13].

During our theoretical investigations of the structure and function of various metalloproteins [17–30], we have tested several strain hypotheses by quantifying the strain and estimating its importance for the function of the protein. We have in no case seen any significant effect of strain in proteins. However, for smaller molecules we have sometimes observed strain, although not very large in energy terms (10–20 kJ/mole). This has given us the opportunity to study how small strained molecules differ from proteins. In this paper, we will review these results.

We will first discuss various definitions of strain. With a clear definition, the strain can be quantified and we can estimate its functional importance. Next, we examine two simple harmonic models, which allow us to draw some general conclusions about strain. Finally, we describe some examples of systems were we have or have not found significant strain.

For simplicity and clarity, we will throughout the article consider only how a protein may strain the coordination sphere of a bound *metal* ion. However, the principles are general and apply to distortions of any group or molecule bound to a protein.

DEFINITION

What is strain? Intuitively and in its well-defined physical sense, something is strained when it is not allowed to attain is natural structure, i.e. when it is physically *distorted* [6]. For example, Comba has defined strain as deformation of a complex caused by interactions between the atoms in it [15]. For a metal bound to a protein, this implies that the geometric preferences of the metal and the protein differ, leading to stress *forces* in both the metal and the protein.

Let us consider a typical example of a strained molecule, cyclopropane. It is strained because it does not assume the typical bond lengths and angles of a normal saturated hydrocarbon. We can take propane as the strainless reference state and by comparing the geometries, we can quantify the effect of strain in bond lengths and angles. Moreover, we can compare the heat of formation of the two compounds and get an estimate of the strain energy. However, this comparison is not fully straightforward, since the two compounds differ in the number of atoms and bonds. Finally, we note that the distortion is caused by the extra C–C

bond, forming a ring.

Thus, for this molecule, it is quite simple to define what we mean by strain. However, when we consider a protein, things start to be more complicated. Clearly, protein strain arises when the properties of a molecule (metal or group) become distorted when bound to a protein. By comparison with the cyclopropane example, two things need to be settled before we have clarified what we mean by protein strain. First, we must specify the strainless *reference state* of the molecule, and second we need to decide *what interactions* (distorting factors) we include in the concept of strain [15].

At least two reference states are conceivable: the same molecule in vacuum or in aqueous solution. The first choice is well-defined and simple to study in theoretical calculation. However, it is harder to study by experiments and it may give rise to some artificial effects if the molecule involves polar or charged groups, since polar interactions are stronger in vacuum than in a protein or in solvent [20].

An aqueous reference state is harder to define, since the concentration and composition has to be specified. If a standard concentration of 1 M is used, the molecules may start to interact and polymerise, giving rise to effects normally not considered as strain, whereas an infinite dilution may lead to dissociation. Moreover, an ionic strength of zero may seem as artificial as vacuum for a biochemical system.

For a metal complex these problems are especially pronounced, because the ligands will most likely be replaced by water ligands at infinite dilution. It is also open to discussion if other ligands (normally present in biological systems) may be allowed to bind in the reference state, if the coordination number should be allowed to change, and if the metal or ligands should be allowed to react with each other.

Moreover, for metal complexes, the composition of the reference molecule is not clear, because some of the native ligands normally come from the protein. We will show in our examples that this choice is crucial. Ideally, we should use ligands that chemically resemble the protein ligands as much as possible. At the same time, they should not contain other chemical or polar groups that may give rise to distorting interactions in the reference state. Therefore, the ligand models should typically consist of the amino-acid side chain, but not the backbone (e.g. imidazole for histidine, acetate for aspartate, CH_3S^- for cysteine, etc.). For the longer side chains (lysine, glutamate, methionine, etc.), the number of carbon atoms in the model can be discussed. Our theoretical results indicate, that one methyl group is normally enough to obtained converged geometries, energies, and spectra [20,31]. It has been argued that even smaller models can be used for energies [32].

Sometimes, an even wider definition of the reference state is used, viz. the typical or ideal geometry of the metal ion with *any* ligands (i.e. not exactly those encountered in the protein) [15]. For example, Williams suggests as the reference state model complexes with freely mobile ligands, e.g. water [11]. However, with such a definition, it is not possible to quantify strain in energy terms (neither by experiments nor by calculations), since we compare different molecules. Moreover, such a definition will include the choice of metal ligands in the strain concept, which is counterintuitive

For these reasons, we use *the same molecule* (e.g. a metal with the same ligands as in the protein) *in vacuum* as the reference state. Yet, the most important point is not to settle the reference state, but rather not to mix results obtained with different reference states.

The second question is related to what we mean by strain, but also to the *cause* of (the explanation to, the mechanisms behind) the strain. In cyclopropane, the extra C–C bond cause the distortions and this is in accordance with our intuitive meaning of strain as a mechanical distortion caused by pushing or drawing in

bonds. However, in a protein, many more processes may be active, e.g. the choice of ligands, electrostatics, hydrogen bonds, solvation effects, dynamics, etc., most of which we do not normally consider as strain.

In molecular mechanics calculations, the interaction between atoms is described by separate energy terms for bonds, angles, dihedrals, electrostatics, and Van der Waals interactions (sophisticated force fields include more types of terms, as well as cross terms) [57]. Based on such a division, Warshel has defined strain as *distortions caused by covalent interactions* (bond, angles, and dihedrals) and possibly also the repulsive part of the Van der Waals interaction [4]. This is close to the intuitive conception of mechanical strain. We have adopted this definition and we will refer to it as *covalent strain*. Thus, we distinguish between distortions caused by covalent strain and those caused by other mechanisms (which we try to identify).

The disadvantage with such a definition is that it is strictly applicable only in molecular mechanics simulations. In other theoretical calculations, we can aim at isolating these effects, but it is not always so easy. In experiments, it is even worse. The alternative view, i.e. to include *all effects* of the protein, is adopted by Gray, Malmström, and Williams in their concept "constrained" in a recent commentary [33]. The disadvantage of such a definition is that is says nothing about the mechanism and that it is counterintuitive.

Finally, a third point has also to be discussed: What is significant strain? This is important because all molecules necessarily acquire slightly different properties when bound to a protein. This is an effect of the trivial fact that a protein is different from vacuum or solution (it has another effective dielectric constant and presents specific electrostatic interactions).

This is most clearly seen for the reduction potential of a metal. It strongly changes when a metal is bound to a protein (even compared to a metal complex with the same first-sphere ligands). For example, the reduction potential of a haem group bound to an octapeptide has a reduction potential that is 300–500 mV lower than that in a protein, and synthetic [4Fe–4S] clusters have reduction potentials that are 500–800 mV lower than those in ferredoxins [34]. However, if we had similar sensitive probes we would have seen the same effects for other properties as well (geometry, chemical potential, etc.).

Therefore, we have to specify what we mean by significant strain. We have used a simple solution: We consider a metal to be significantly strained if the strain energy is *larger than normal*, i.e. larger than for most other metalloproteins. We prefer to discuss strain in *energy* terms (instead of geometry, for example) because all processes in chemistry are governed by the (relative free) energy, and a large change in geometry does not necessarily imply a large energy [22,28]. Moreover, we demand that an important constraint should have a *significant effect on the function* of the protein. Otherwise, the strain may be accidental.

QUANTIFY STRAIN

In order to test strain hypotheses, it is necessary to quantify the effect of strain. Once the concept strain has been defined, this can be done, at least in principle. In this section we will discuss how it can be done and point out possible pitfalls.

With our reference state, i.e. the molecule in vacuum, the reference properties (geometry, energy, etc.) are easily obtained by quantum chemical methods. We do not intend a lengthy discussion about the best available quantum chemical methods. We have used the B3LYP method [35], which has been shown to be the best widely available density functional [36–38]. Density functional methods are known to give excellent results for most systems (especially transition metal complexes) at a rather modest cost [37,38] and must be considered the method of choice for most systems of biologi-

cal interest.

A basis set of split-valence quality with polarisation functions on non-hydrogen atoms (e.g. 6–31G* [39]) gives excellent geometries. Typically, bond lengths between hydrogen and first-row atoms are reproduced within 1 pm, whereas bonds to transition metals are systematically overestimated by 2–7 pm [28,30]. For weak interactions, e.g. metal–metal distances the error can be larger [28,29]. Energies calculated with this method are usually reasonably accurate [40]. However, for very accurate results, they could be improved by single-point calculations using either larger basis sets (density functional methods are usually converged at the triple-ζ level with double polarisation functions on all atoms [36–38]) or with more accurate methods, e.g. CASPT2, CCSD(T), or G2 [41–43]. It should also be noted that if weak intermolecular interactions are involved, a method which explicitly treats dispersion should be used, e.g. MP2 [44].

Once the theoretical method has been chosen, the properties in vacuum can be calculated. They should be compared with those in a protein, which can be obtained either from experiments or from other calculations. If accurate experimental data is available, this is of course best. However, it must be remembered that some of differences between the vacuum and protein properties may then be caused by errors in the theoretical method and not by strain. This possible source of error can be compensated for if calibrated theoretical results are available.

If experimental data are not available or if they are too inaccurate, the structure of the metal (or any other property) in the protein has to be estimated by theoretical methods. This is far from trivial and new methods are still developed. Several different levels of sophistication have been used and the method of choice depends on the property of interest.

The lowest level is to assume that the protein has little influence on the properties and calculate them directly in vacuum on an appropriate model system. This, of course, implies that strain in Warshel's sense is not important. It has been suggested, for example, that the protein has a limited influence on reaction mechanism, provided that all residues involved in the mechanism are included in the calculations, that there are no strong interactions (e.g. hydrogen bonds) between the active site and the rest of the enzyme, and that the total charge of the model complex is zero [37,38].

The next level of approximation is to include the protein as a dielectric continuum with a specified dielectric constant (typically 2–16) [45,46]. This method has been used for reaction energies in the protein and the correction is typically small (~4 kJ/mole) if the model complex is neutral [37,38]. It can be refined by adding another continuum with the dielectric constant of water (~80) outside the protein and modelling each protein atom by a fractional charge. Such methods have been used for the calculation of reduction potentials in proteins and for quantum chemical calculations and geometry optimisations [47–52]. In general, the results are quite good. For example, it has been shown that the reduction potential of related proteins and mutants can be predicted with an average error of 50 mV if the crystal structure is known [52].

The alternative to these continuum models is to use an atomic model of the protein and solvent. A simple point-charge model of the protein without any dielectric continuum has been used for electronic spectra or reductions potentials [31,50,53,54]. Warshel and coworkers have extensively used a Langevin dipole model of water together with polarisable point charges for the protein atoms for the calculation of reduction potentials, reaction energies, etc. in the protein [4,52,55]. Most molecular mechanics methods also depend on an atomic description of the protein and they have successfully been used for the study of many properties of proteins, including strain energies, dynamics, and free energies [56–58]. The main problem

with such methods is the limited accuracy of current classical force fields combined with severe problems of convergence for the simulation times attainable at present [57].

A way to circumvent these problems is to combine molecular mechanics simulations with more accurate quantum chemical methods for a small system of interest (e.g. the active site). This yields the combined quantum chemical and molecular mechanics methods (QC/MM), of which many different approaches are available [25,59–62]. In these, you can use the same quantum chemical method as in vacuum. Thereby, artefacts caused by systematic errors in the theoretical method are minimised. QC/MM methods have been used to calculate structures, strain energies, and functional properties of metal sites in proteins [20,24–26,29, 59–62]. Very recently, we have modified this technique to use crystallographic raw data (structure factors) as a restraint for the protein structure [63]. Thereby, we ensure that errors in the quantum chemical or molecular mechanics methods do not distort the structure away from the experimental one. Thus, we obtain a structure that is an optimum compromise between experiments and theory.

If you prefer to use aqueous solution as the reference state, such properties could be calculated by modelling the surrounding solvent in a similar way as the protein [58]. Methods of almost all the types discussed above have been used for this. It should be noted, however, that hydrogen bonds between the molecule of interest and water often strongly influence the properties of the molecule, and therefore often need to be explicitly included in the theoretical calculations.

Up to now we have ignored the problem of how to distinguish between various causes of the distortions. If we use Gray, Malmström, and Williams' definition [33], all differences between the reference and protein calculations are attributed strain. However, if we want to look somewhat deeper into the cause of the distortions and use Warshel's restricted definition of strain [4], the results are not so easily interpreted. In pure molecular mechanics methods, the various contributions to the energy are separated in the calculations and we can directly read off the strain as the bond, angle, and dihedral terms or at least we can shut off each contribution in separate calculations.

In quantum chemical calculations, this is harder. In our QC/MM calculations, we have separated the effect of covalent strain by performing separate calculations in which the covalent links between the direct metal ligands and the protein have been removed [20,24]. The resulting difference between these calculations and those of normal QC/MM calculations is a measurement of covalent strain (as opposed to electrostatic, hydrogen bond, and solvation effects).

Finally, it should be noted that optimisation methods give structures and energies at 0 K. Strictly speaking, however, the chemically relevant quantities are *free* energies and structures at ambient temperatures. There are theoretical methods to calculate also these quantities. For example, molecular dynamics simulations directly reflect the dynamics of the system and they, or Monte Carlo simulations, can be used to obtain free energies by perturbation methods [56,57].

These methods are in principle applicable also with a quantum mechanical energy function, but the cost is normally prohibitively large. Alternatively, free energies (together with zero-point energies) can be estimated from the vibrational frequencies of the molecule. In general, such corrections are small and rather insignificant [37,38]. For example, the inner-sphere reorganisation energy of a realistic blue-copper model changes by 6 kJ/mole (out of 63 kJ/mole) when zero-point and thermal corrections are included. However, for structures the dynamic effect at ambient temperatures may be appreciable. For example, the length of the weak Cu–S_{Met} (methionine sulphur) bond in the

blue copper proteins increase by at least 10 pm when the temperature is increased from 0 to 300 K [18].

HARMONIC MODELS

In this section we will examine two simple systems with opposing forces. Although the models are oversimplified, they illustrate several important concepts about strain in a mathematically transparent way.

First, consider the system in Figure 1. It represents a bond between a metal and a ligand, for example the supposedly strained Cu–S_{Met} bond in the blue copper proteins. We assume that without the protein, the potential of this bond, as a function of the bond length r, follows a harmonic potential with the equilibrium bond length r_{10} and the force constant k_1.

$$V_1(r) = \frac{k_1}{2}(r - r_{10})^2 \qquad (1)$$

Similarly, we assume that without the metal ion, there is a cavity in the protein, the size of which also follows a harmonic potential with an equilibrium size r_{20} and a force constant k_2.

$$V_2(r) = \frac{k_2}{2}(r - r_{20})^2 \qquad (2)$$

When the metal is bound to the protein, there will be a conflict if $r_{10} \neq r_{20}$, and strain will build up in both the protein and the metal[1]. Equilibrium will attain when the forces of the protein and the metal are equal but opposite (i.e. when their sum vanishes). Since the force is the negative of the first derivative of the potential with respect to r, they can easily be derived in this simple model (c.f. Hook's law):

$$F_1(r) = k_1(r - r_{10}) \qquad (3)$$

$$F_2(r) = k_2(r - r_{20}) \qquad (4)$$

Therefore, we can directly find the equilibrium bond length r_{eq} as a function of r_{10}, k_1, r_{20}, and k_2:

[1] This model is not fully realistic, because the potentials of the free metal and protein may change when they bind. Strictly speaking, we should have used different force constants and equilibrium distances in the reference states and in the coupled state. However, for clarity, we ignore this effect.

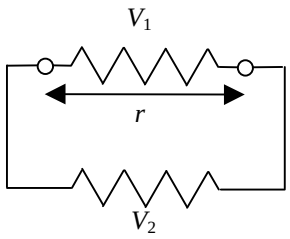

Figure 1. Schematic picture of the harmonic model in Eqn. (1)–(2).

$$r_{eq} = \frac{k_1 r_{10} + k_2 r_{20}}{k_1 + k_2} \qquad (5)$$

By comparing r_{eq} with r_1 and r_2, we can see how much the bond lengths will distort from the strainfree values. In particular, the quotient of the distortions of the bonds in the protein is given by:

$$\frac{r_{eq} - r_{10}}{r_{eq} - r_{20}} = -\frac{k_2}{k_1} \qquad (6),$$

i.e. the quotient of the corresponding force constants. Thus, the most flexible interaction will distort most, which is fully intuitive.

This relation propagates also to the corresponding strain energies. The strain energy of the metal is $V_1(r_{eq})$–V_1 (r_{10}) and a similar relation applies for the protein. Again, we see that the quotient of the strain energies is given by the quotient of the corresponding force constants:

$$\frac{V_1(r_{eq}) - V_1(r_{10})}{V_2(r_{eq}) - V_2(r_{20})} = \frac{k_2}{k_1} \qquad (7)$$

Thus, the more flexible part (metal or protein) will acquire the largest strain energy.

This model shows that in general, *both* the metal and the protein will distort when they interact and the relative distortion is determined by relative size of their force constants. Thus, among Williams' four cases of an energised metal site [11], the typical case is the induced fit or rack, where both the protein and the metal are distorted. The entatic and induced matrix states can be seen as limiting cases when the force constant of the protein is much larger than that of the metal or vice versa. The meaning of

"much larger" is not discussed by Williams (and is harder to define when all bonds between the metal and the protein are considered), but it is clear that the decision is based on observed distortions, rather than on energies or force constants.

This analysis suggests that we shall compare the magnitude of the force constants of various interactions in a protein and a metal site. They can be found in the force fields of any common biochemical simulation package. We have used those of the Amber force field [64].

The harmonic force constant of a covalent bond is typically between 600 (S–S) and 2600 (carboxylate C–O) kJ/mole/Å^2. It is large for charged, polar, and aromatic groups, and smaller for second-row atoms. Bonds to metals are weaker, having force constants ranging between 400 kJ/mole/Å^2 for a strong Cu–S_{Cys} bond and 40 kJ/mole/Å^2 for a weak Cu–S_{Met} interaction [18]. The force constants of angles are 120–340 kJ/mole/Å^2 in normal molecules and 40–100 kJ/mole/Å^2 around metals. Those of dihedral angles in aromatic systems are similar in magnitude, 20–100 kJ/mole/Å^2, whereas they are smaller in non-aromatic systems, <8 kJ/mole/Å^2.

The effective force constants of non-bonded interactions are harder to estimate, since they depend on the distance between the interacting atoms. However, for a Van der Waals interaction, we may get an estimate of the effective force constant from the second derivative of the Lennard–Jones potential at its minimum. For the Amber force field, it varies between 2 and 8 kJ/mole/Å^2. However, at short distances it becomes appreciably larger.

The electrostatic interaction is even harder to quantify, since it depends on the charges of the interacting atoms as well as their distance. Moreover, there is no optimum distance, but the energy decreases linearly with the distance between two charges, and as r^{-3} between two dipoles. The interaction is also stronger in vacuum than in solution or in a protein. The best we can do is to consider a typical example, e.g. the water dimer, which has a force constant of ~40 kJ/mole/Å^2 at the minimum. This estimate includes both electrostatic and Van der Waals interactions, and at the same time estimates the strength of a typical hydrogen bond.

This inventory gives us the opportunity to analyse relative force constants for some systems, giving us a deeper understanding in the relative strength of the opposing forces. First, let us consider cyclopropane, for which strain is caused by an extra covalent C–C bond and the effect of strain is seen in the distorted angles and dihedrals. This agrees with our inventory: bonds are about five times more rigid than angles and more than hundred times more rigid than the torsional angles. Moreover, the C–C–C angles cannot be improved by changing the bond lengths, since they are part of a ring. This shows that covalent rings are effective in inducing strain.

For a metal bound to a protein, things are different. As we saw above, metal–ligand bonds are weaker than covalent bonds, but stronger than angles. However, the local environment in a protein is dictated by non-aromatic torsions (of the side chains) and by Van der Waals interactions. They are weaker than metal–ligand bonds and normally allow for quite appreciable movements of the ligands (~100 pm). Therefore, it is unlikely that a protein may dictate moderate changes in the metal geometry. Several other authors have arrived at the same conclusion [4–6].

For larger changes, however, the protein backbone has to move, which involves secondary structure elements and therefore the possible disruption of many hydrogen bonds and a change in the packing and solvent accessibility of hydrophobic groups. These cooperative effects of the protein fold might give rise to appreciable energies and forces (but only after all the weaker, local, interactions have distorted fully), and they explain how proteins can dic-

tate metal ligands and protect metal sites from unwanted ligands. However, these effects are not covalent strain (i.e. they are not caused primarily by covalent interactions). Moreover, there is no distorting *force* for these effects.

We have estimated total strain energies in the blue copper proteins, supposed to be extraordinary rigid [6,10,11,16,17,65], as an effect of possible constraints in the Cu–S_{Met} bond [18]. The result showed very modest strain energies for sizeable changes in the geometry, e.g. 0.2–2.5 kJ/mole for a 20-pm change in the bond length, and 5 kJ/mole for a 50-pm change. This illustrates that even a rigid protein is locally flexible.

Next, we consider the slightly different model in Figure 2. In this case, we assume that the protein is rigid and look at a metal bound to the protein by two bonds, the potentials of which follow Eqns. (8) and (9), respectively.

$$V_3(r) = \frac{k_3}{2}(r_3 - r_{30})^2 \qquad (8)$$

$$V_4(r) = \frac{k_4}{2}(r_4 - r_{40})^2 \qquad (9)$$

In our Cu–S_{Met} example, the atoms in Figure 1b can be interpreted as Cu in the middle, S_{Met} at the left side and another ligand atom, e.g. S_{Cys} on the right side. The only difference to the previous model is that the lengths of the two bonds may differ, r_3 and r_4. Furthermore, we assume that the two bonds remain parallel and that the sum of the two bonds are constant, r_0 (the protein is rigid):

$$r_3 + r_4 = r_0 \qquad (10).$$

This applies when there are no further forces and $r_{30} + r_{40} < r_0$, i.e. when the bonds are stretched. If the bonds are compressed, the angle between the three atoms will also change.

With the same argument as above, equilibrium will obtain when the sum of the corresponding forces vanishes. This gives the following two equilibrium bond lengths:

$$r_{3eq} = \frac{k_3 r_{30} + k_4(r_{40} - r_0)}{k_3 - k_4} \qquad (11)$$

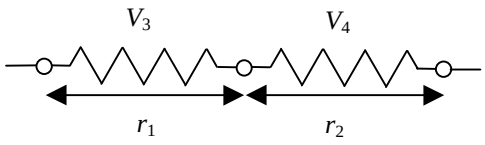

Figure 2. Schematic picture of the harmonic model in Eqn. (8)–(9).

$$r_{4eq} = \frac{k_4 r_{40} + k_3(r_{30} - r_0)}{k_4 - k_3} \qquad (12)$$

Just as in the previous model, we will find that the relative geometric distortion of the two bonds and the relative strain energy will be related to the quotient of the corresponding force constants:

$$\frac{r_{3eq} - r_{30}}{r_{4eq} - r_{40}} = -\frac{k_4}{k_3} \qquad (13)$$

$$\frac{V_3(r_{3eq}) - V_3(r_{30})}{V_4(r_{4eq}) - V_4(r_{40})} = \frac{k_4}{k_3} \qquad (14).$$

This model shows that if a metal site is constrained, there must always be distortions in at least *two* bonds.

For example, it is impossible that *only* the Cu–S_{Met} bond in the blue copper proteins is strained [66,67]. There must also be strain in some of the other three copper ligands. In fact, the resultant of the strain forces of the three strong ligands should equal the negative of the strain force of the methionine ligand. Even if the force constants of the former ligands are 4–10 times larger than that of the methionine ligand [18], the forces on them would be appreciable, because they form an approximate trigonal plane, perpendicular to the methionine ligand. A simple calculation based on the crystal structure of plastocyanin [68] indicates that the force on each of the strong ligands should be 2–3 times that on the methionine ligand. Consequently, the distortion of each of the strong bonds should be at least 20% of that of the Cu–S_{Met} bond. Such distortions are not observed, which support our argument below that there is in fact little strain in the Cu–S_{Met} bond.

This model also illustrates the importance

of cyclic systems to introduce strain in a metal: the metal must be kept fixed at two positions in order to induce strain. This is most easily achieved in cyclic systems, where the angular and torsional freedom is restricted by aromaticity (as in a porphyrin) or bulky side groups (as in many inorganic models).

STRAIN AND ACTIVATION ENERGIES

It has been argued that strain, or more generally, a destabilisation of the substrate, directly decreases the activation energy [69,70]. The argument is illustrated in Figure 3a. Without the enzyme, the substrate S has to overcome a transition state T with an activation energy E_1 before reaching the product P. However, by destabilising the substrate when it is bound to the enzyme (ES), it comes closer to the transition state, and the activation energy would be lowered (E_2). Thus, the binding energy of the enzyme is partly used to promote the reaction.

Unfortunately, this argument is incomplete. The activation energy, which determines the rate of the catalysed reaction, is the difference in energy between the highest transition state along the reaction path and the reactant (substrate or intermediate) with lowest energy before that transition state [3]. Thus, if we include the free substrate and product, together with the transition state of the uncatalysed reaction, (all at infinite separation from the enzyme, E+S, E+T, and E+P) in the energy diagram (Figure 3b), we see that, if the enzyme does not lower the transition state, the activation energy of the full reaction will still be E_1 (provided that the energies of the transition states for the binding of the substrate to, T_1 or dissociation of the product from the enzyme, T_2, are not higher). Thus, destabilisation of the substrate–enzyme complex does not automatically lead to catalysis. Otherwise, we could reduce the activation energy simply by dividing the reaction into many steps, each with a small activation energy.

Instead, the important thing is the energy of the transition state relative to that of the lowest intermediate. If it is lowered as E_3 in Figure 3b, the reaction rate will increase. This could in principle be done by a rigid site, complementary to transition state, but this comes close to the normal source of catalytic power, the preferential stabilisation of the transition state [3, 6]. Of course, it is also important that the enzyme–substrate complex (ES) is not too sta-

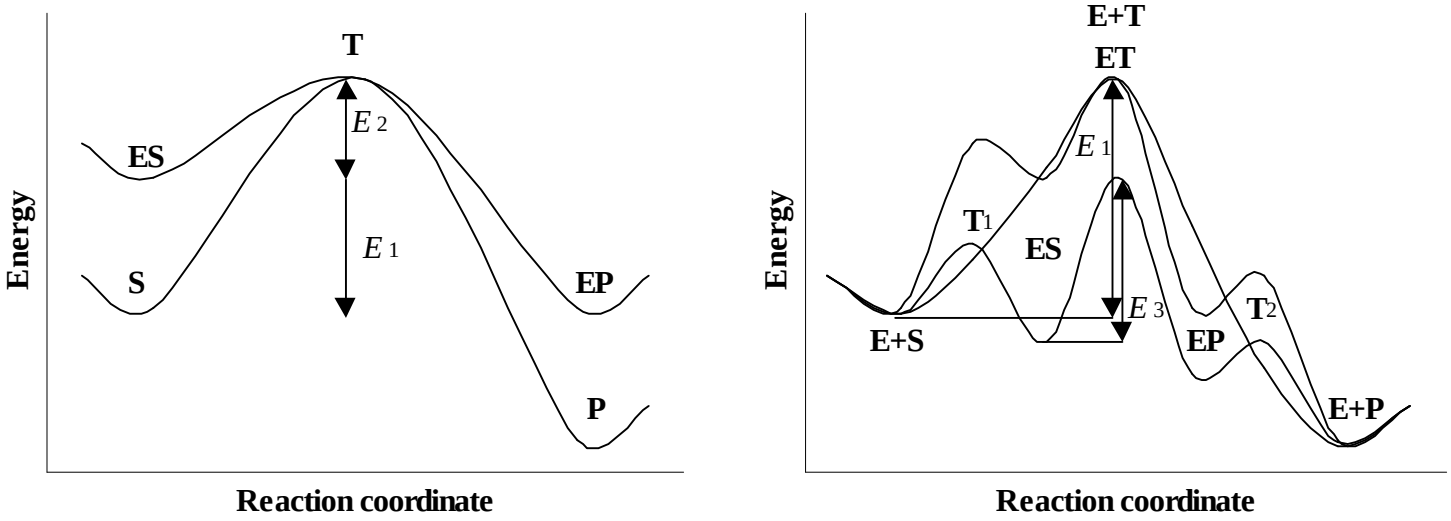

Figure 3. Two energy profiles of the S→P reaction in solution and in an enzyme. The left picture (a) shows the isolated reaction and how the activation energy has been suggested to decrease by destabilisation of the enzyme–substrate complex (ES) [70]. The right picture (b) shows that if the complete reaction is considered, there is no gain from such a mechanism, unless the energy of the transition state is lowered.

ble, because it normally has the lowest energy before the transition state.

STRAIN IN BIOLOGICAL SYSTEMS

In this section we will examine four systems for which strain has been suggested to play an important role. We will show that in all cases, covalent strain (in the sense of Warshel [4]) is small in energy terms and of little functional value. However, we will also discuss two systems where covalent strain is significant and has a clear-cut function. It should be noted that these are only a few examples from our investigations. The list could be elongated, e.g. with myoglobin (discrimination between CO and O_2 by strain or electrostatic stabilisation) [9,110–112] and vitamin B_{12} enzymes (the mechano-chemical trigger mechanism) [7,113], but the results are similar.

Blue copper proteins

The blue copper proteins are a group of electron transfer proteins characterised by a number of unusual properties, e.g. a bright blue colour, a narrow hyperfine splitting in the electronic spin resonance (ESR) spectra, and high reduction potentials [71–73]. Moreover, crystal structures of the oxidised form of these proteins show a structure distinct from what is normally observed for small inorganic complexes (tetragonal to distorted octahedral [74]): The copper ion is bound to the protein in an approximate trigonal plane formed by a cysteine thiolate group and two histidine nitrogen atoms. The coordination sphere in most blue copper sites is completed by one or two axial ligands, typically a methionine thioether group [24,71–73]. Such a geometry is similar to what can be expected for Cu(I) complexes, and reduced blue copper proteins have copper coordination geometries that are very close to those of the oxidised proteins [72,73,75]. Naturally, this is a functional advantage for an electron transfer protein; if the two oxidation states of the copper centre have similar structures, the reorganisation energy will be low, and the rate of electron transfer will be high [76].

These unusual properties of the oxidised form of the blue copper proteins have traditionally been explained by protein strain: It has been suggested that the rigid protein forces the Cu(II) ion to bind in a geometry more similar to the one preferred by Cu(I). In fact, the blue copper proteins have been the typical example of both the entatic state [10,11,65] and the induced-rack hypotheses [12,13,16]. Recently, this suggestion has been challenged [17,66], leading to some lengthy debate [27,33,67,77] and a new formulation of the induced-rack hypothesis [78,79]. This debate nicely illustrates the importance of using the same definition of strain.

In order to test the strain hypotheses for the blue copper proteins, we optimised the geometry of $Cu(imidazole)_2(SCH_3)(S(CH_3)_2)^+$ as a realistic model of the prototypical $Cu(His)_2$-CysMet blue copper centre using the density functional B3LYP method [17]. The results in Figure 4 and Table 1 show that the optimised geometry is virtually identical to the one observed experimentally in the blue copper proteins. Almost all bond lengths and bond angles around the copper ion are within the range ob-

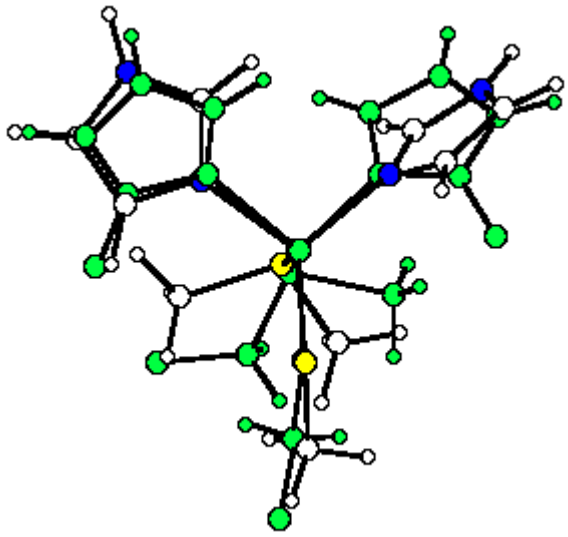

Figure 4. A comparison of the optimised structure of $Cu(imidazole)_2(SCH_3)(S(CH_3)_2)^+$ [17] and the crystal structure of plastocyanin (shaded) [68].

served in crystal structures, and most of them are close to the average values for the proteins. It should be noted that no information from the crystal structure has been used to obtain these structures; they are entirely an effect of the chemical preferences of the copper ion and its four ligands. Similar results were obtained for two other groups of blue copper proteins, nitrite reductase and stellacyanin [19,53] (Table 1). These results clearly show that the cupric blue copper site is not significantly strained compared to the vacuum structure with the same ligands.

Further calculations showed that the unusual trigonal geometry in the blue copper proteins is caused by the strong interaction between the Cu(II) ion and the cysteine thiolate ligand, where much charge is transferred to the copper ion, giving it significant Cu(I) character [53,80]. Moreover, we have tried to quantify the protein strain by optimising the geometry of the copper site also inside the protein using our QC/MM geometry optimisation program, both with and without the covalent bonds between the protein and the copper ligands [20]. With the bonds intact, the protein structure is destabilised by 33–66 kJ/mole in vacuum. This is similar to what is found in other proteins tested with the same method, viz. alcohol dehydrogenase (both the catalytic and structural zinc ions), rubredoxins, and [2Fe–2S] ferredoxins [23–26,29]. If the bonds are broken, the energy decreases by ~25 kJ/mole, which is an estimate of the covalent strain in the blue copper site. This is slightly lower than for the structural zinc ion in alcohol dehydrogenase, the only other site investigated with the same method [24].

Even more interesting, we have shown that the inner-sphere reorganisation energy of the copper site (which, together with the reduction potential and the electronic coupling matrix element, determines the rate of electron transfer for the site [76]) actually *increases* by covalent strain (i.e. the reaction is counteracted by strain) [20]. This has also been observed experimentally [81]. Thus, our investigations have shown that the blue copper proteins are not more strained than other metalloproteins, that the strain energy is modest, and that covalent strain has no functional significance; in short, the blue copper site is not strained in our sense of strain.

Does this mean that the blue-copper site is not entatic? Of course not. According to Williams, a metal site is entatic if the protein structure without the metal is the same when the metal is bound and if the geometry of the

Table 1. Comparison of the geometry of optimised models and crystal structures of blue copper proteins [17,19,53]. *Ax* is the axial ligand and φ the angle between the S_{Cys}–Cu–*Ax* and N–Cu–N planes.

Model	Distance to Cu (pm)			Angle subtended at Cu (°)				φ
	S_{Cys}	N	*Ax*	N–N	S_{Cys}–N	S_{Cys}–*Ax*	N–*Ax*	
$Cu(imidazole)_2(SCH_3)(S(CH_3)_2)^{+a}$	218	204	267	103	120–122	116	94–95	90
Plastocyanin oxidised	207–221	189–222	278–291	96–104	112–144	102–110	85–108	77–89
$Cu(imidazole)_2(SCH_3)(S(CH_3)_2)$	232	214–215	237	109	105–108	115	107–113	89
$Cu(imidazole)_2(SCH_3)(S(CH_3)_2)^{b}$	227	205–210	290	119	112–120	99	100–101	88
Plastocyanin reduced	211–217	203–239	287–291	91–118	110–141	99–114	83–110	74–80
$Cu(imidazole)_2(SH)(S(CH_3)_2)^{+c}$	223	205–206	242	100	97–141	103	95–126	62
Nitrite reductase oxidised	208–223	193–222	246–270	96–102	98–140	103–109	84–138	56–65
$Cu(imidazole)_2(SCH_3)(OCCH_3NH_2)^{+a}$	217	202–206	224	103	122–125	113	92–95	88
Stellacyanin oxidised	211–218	191–206	221–227	97–105	116–141	101–107	87–102	82–86

[a] Trigonal structure
[b] The Cu–S_{Met} bond length was constrained to 290 pm.
[c] Tetragonal structure

metal in the protein differ from the one in model complexes with freely mobile ligands [11]. Apparently, both these premises are fulfilled for the blue copper proteins (in fact, there some differences between the apo- and holoprotein [82], showing that it is open to discussion how large changes are allowed) and therefore the proteins are entatic and then also constrained in the sense of Gray, Malmström and Williams [33]. However, as was discussed above, this does not say anything about the cause of the unusual structure, nor is it possible to quantify this strain in energy terms.

It is clear that both the entatic state and the induced-rack hypotheses in their original formulations included components of covalent stain [13,10,65]. Our calculations show that this mechanism is not active in the blue copper proteins. Instead, the unusual structure and the low reorganisation energy are caused by the choice of copper ligands, in particular the cysteine thiolate ligand [80]. In other words, the reduced and oxidised proteins attain very similar structure because the metal wants it, not because the protein forces it upon the metal. Thus, we have shown a new mechanism for the catalytic efficiency of these proteins. However, they are still entatic, because this theory is defined purely on experimental observations and does not say anything about the mechanism behind the observation. This shows the strength of our definition

The blue-copper site was assumed to be strained because its structure differed from that of inorganic models. However, no small inorganic models are available with freely mobile ligands of exactly the same type as found in the blue copper proteins [83,84]. This is caused by many practical problems in the synthesis of such complexes [85], most prominently that thiolates are oxidised by Cu(II). This illustrates the risk of using a complex with different ligands as a reference state of the metal. By such a definition, the blue copper site is unnatural, but the difference is not caused by strain but by the choice of ligands.

Naturally, the protein has other functions than providing the proper ligands [17,27]. For example, it protects the copper site against water [11,17,33], which could come in as an additional or replacing ligand to copper, thereby stabilising a more tetragonal structure with a higher reorganisation energy [53]. Moreover, it also affects the local dielectric milieu of the copper ion, thereby increasing the reduction potential of the copper site [78]. However, this is not a mechanical deformation and therefore not what people normally call strain. Furthermore, the same effect on the reduction potential is seen in all redox-active metal proteins.

Recently, it has been proposed that the Cu(I)–S_{Met} bond is the only (covalently) strained structural parameter of the blue copper site [66,67], and that this constraint would fix the reduction potential of the site [78,79]. This suggestion is partly based on the fact that this bond is shorter in calculated structures (~235 pm) than in proteins (~290 pm), c.f. Table 1. However, when comparing calculated and experimental structures, there is always the possibility that the differences are caused by errors in the calculations. We have shown that the Cu–S_{Met} bond is extremely flexible [17,22]: It costs only 4 kJ/mole to change it to the distance found in the protein, i.e. well within the error limit of the method. Moreover, every improvement of the method, basis set, model system, solvation effect, etc. tend to increase the bond length [17,40], as do the dynamics at ambient temperatures [18]. Thus, it is far from clear that there is any discrepancy between calculations and experiments for this bond, but if there is any, it is extremely small in energy terms.

Furthermore, we have examined the possible effect of any constraints in this bond on the reduction potential of the copper site. Irrespectively of the effective dielectric constant of the protein, the effect of constraints in the Cu–S_{Met} bond is less than 70 mV [22]. If the second axial ligand, present in some proteins, is also

taken into account and removal of axial ligands is considered, the possible effect is larger, up to 140 mV. Still, this range is quite small considering that the reduction potentials of blue copper proteins vary between 180 and ~1000 mV. The effects of solvation and oriented dipoles around the copper site are most likely more important [86,87]. It is not even probable that the observed differences in the reduction potentials are caused by variations in the Cu–S_{Met} bond length. Unambiguous effects are only seen when the methionine ligand is removed or replaced by other ligands [88], but this is an effect of ligand substitution and not of covalent strain.

This reduces the discussion about a strained Cu–S_{Met} bond to semantics, i.e. what is significant strain and what is a significant change in reduction potential. From crystal and NMR structures, it obvious that the Cu–S_{Met} bond length varies among proteins (260–295 pm for sites with the normal ligands $His_2CysMet$) [33], more than what can be assigned to the experimental uncertainty. However, our calculations show that this variation corresponds to less than 4 kJ/mole in energy terms. Is this a significant strain energy or is it similar to what you would find for other geometric parameters (although the geometric differences would be much smaller, because other bonds are less flexible)? Is it even meaningful to discuss differences in the bond length of such a flexible bond, which show very large dynamic variations at ambient temperature [18]?

Desulforedoxin

Iron–sulphur clusters are ubiquitous in biology and one of the three common electron carriers in proteins, together with blue copper proteins and cytochromes [89,90]. The simplest iron–sulphur cluster is the rubredoxin site, consisting of an iron ion bound to four cysteine thiolate groups. Normally, these sites are nearly tetrahedral, with S–Fe–S angles in the range 104–117°, i.e. similar to what is found for inorganic (104–115°) and theoretical (106–112°) models of this site [29,91]. However, in the desulforedoxins, a group of rubredoxins from the bacteria *Desulfovibrio*, the variation is appreciably larger, 103–122° [8c]. The reason for this variation is that two of the cysteine ligands come directly after each other in sequence,

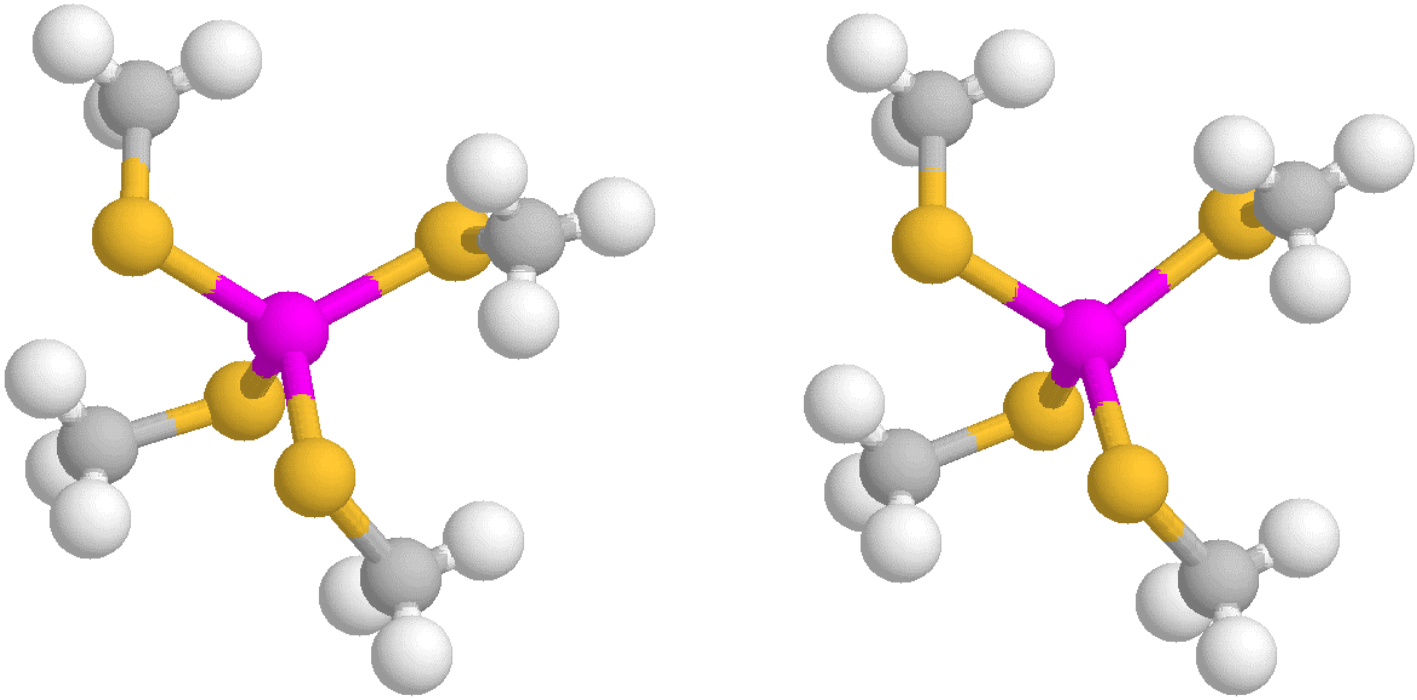

Figure 5. The optimum structure of $Fe(SCH_3)_4^-$ with (left) and without one S–Fe–S angle (the upper one) constrained to 122° (111° in the unconstrained structure) [29]. The energy difference of the two structures is 3.2 kJ/mole.

which for steric reason gives rise to the largest angle. This has been taken as evidence that the site is strained by the protein to a catalytic advantage [8c].

In order to test this suggestion, we have optimised the geometry of $Fe(SCH_3)_4^{-/2-}$ with one of the S–Fe–S angles constrained to 122° (Figure 5). This increased the energy of the complex (compared to the unconstrained structure), but only by 3 kJ/mole in both the reduced and oxidised states [29]. This is a measure of the strain energy (relative to the optimum vacuum geometry) and it shows that the strain is very small in energy terms. Moreover, the calculated inner-sphere reorganisation energy of the constrained complex is 4 kJ/mole *higher* than for the unconstrained complex, so the constraint does not enhance the rate of electron transfer. Neither does the reduction potential change significantly, since the energy of reduced and oxidised forms increased by the same amount when constrained. Therefore, it seems that this larger angle, which undoubtedly is caused by the protein, does not affect the properties of the iron–sulphur site in any significant way.

This analysis shows that a large observed difference in a geometric parameter does not necessarily imply that it is important for the function. Instead, it may reflect a small force constant (the site is flexible) so that the difference in energy terms is small and therefore of minor functional importance. To get a measure of the importance of the geometric effect, the strain energy has to be estimated and the functional implications of it has to be investigated.

The immunochromic effect

The third example comes from a quite different system. Five years ago, results were presented in Nature showing that the absorption of a Cu(I) bis-bipyridine complex (Figure 6) is red-shifted by up to 55 nm when bound to antibodies raised against a similar silicon bis-biphenyl complex (spirosilane) [8a]. It was suggested that the reason for this "immunochromic" effect is that the antibody compresses the Cu–ligand bonds by about 16 pm, i.e. the difference between the Si–C (187 pm) and the Cu–N bonds (203 pm) in the free spirosilane and copper complexes, respectively [8a]. The proposal was supported by quantum chemical calculations, showing that a 19-pm contraction of the Cu–N bond length could give rise to a 45-nm spectral red-shift in one of the absorption lines (calculations on the most realistic model gave only a 15-nm shift, however). The remaining difference was attributed to solvent effects.

Let us analyse this superficially attractive argument. First, we note that the authors use the same reference state as we, i.e. the optimum geometry of the copper complex in vacuum. Using this reference, they estimate the cost of compressing the Cu–N bonds to 50–63 kJ/mole. This is a very high energy, compared to the effects we have observed, e.g. 4 kJ/mole for the $Cu–S_{Met}$ bond in the blue copper proteins. Logically, this energy must be taken from the binding energy of the ligand to the antibody – it corresponds to a reduction of the binding constant by 10^8–10^{11}, i.e. quite an unrealistic strain energy.

Second, it is unlikely that a too small cavity would compress *only* the Cu–N bonds. A more

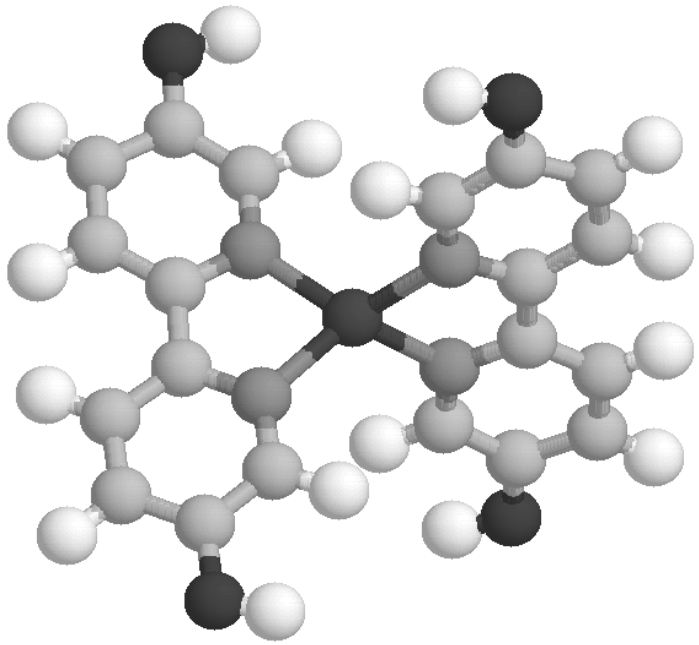

Figure 6. The Cu(I) bis-bipyridine complex suggested to be strained by an antibody [8a].

realistic model of a tight binding site is to optimise the structure of the copper complex constraining the distance between the two most distant atoms in the structure. This results in a structure where the strain energy is reduced to 20 kJ/mole and where the Cu–N bonds are compressed by only 9 pm. Thus, a rigid protein would shorten the Cu–N bonds by only half of the amount suggested. Most importantly, however, the *antibody* will also distort and this distortion will be substantial since, as we discussed above, a protein has numerous degrees of freedom, which are appreciably more flexible than the Cu–N bonds [17]. The actual effect of the protein is impossible to estimate without a detailed structure of the antibody, but considering that the Cu–N bonds are fairly strong, the major change is expected to be found in the protein.

Consequently, compression of the Cu–N bonds does not seem to be a credible cause of the observed red shifts; instead an alternative reason has to be found. However, a 55 nm spectral shift for a ligand bound to a protein is not unprecedented. For example, it is well-known that the absorption peaks of the three colour receptors in the goldfish eye are 455, 530, and 625 nm. This 170-nm variation is caused by small differences in the proteins, mainly in three hydroxyl groups near the retinal chromophore [3]. Moreover, quantum chemical calculations have shown that a protein may change the absorption energy of a chromophore by at least 2000 cm^{-1} (corresponding to ~50 nm at the relevant wavelengths) [31,53]. Thus, a more probable reason for the immunochromic effect is that the antibody presents charged and polar residues near the chromophore, which affect the spectrum by their electric field.

Actual strain in cytochromes

Our fourth example involves a system where covalent strain actually is significant, both in terms of energy and function. This shows that we really can find and quantify strain by our methods, i.e. we have not defined away this possibility. The example again comes from bioinorganic chemistry, viz. from the cytochromes, the third widely used group of electron carriers. In these proteins, the electron is carried by a haem group, i.e. an iron ion bound to a porphyrin ring. Two axial ligands from the

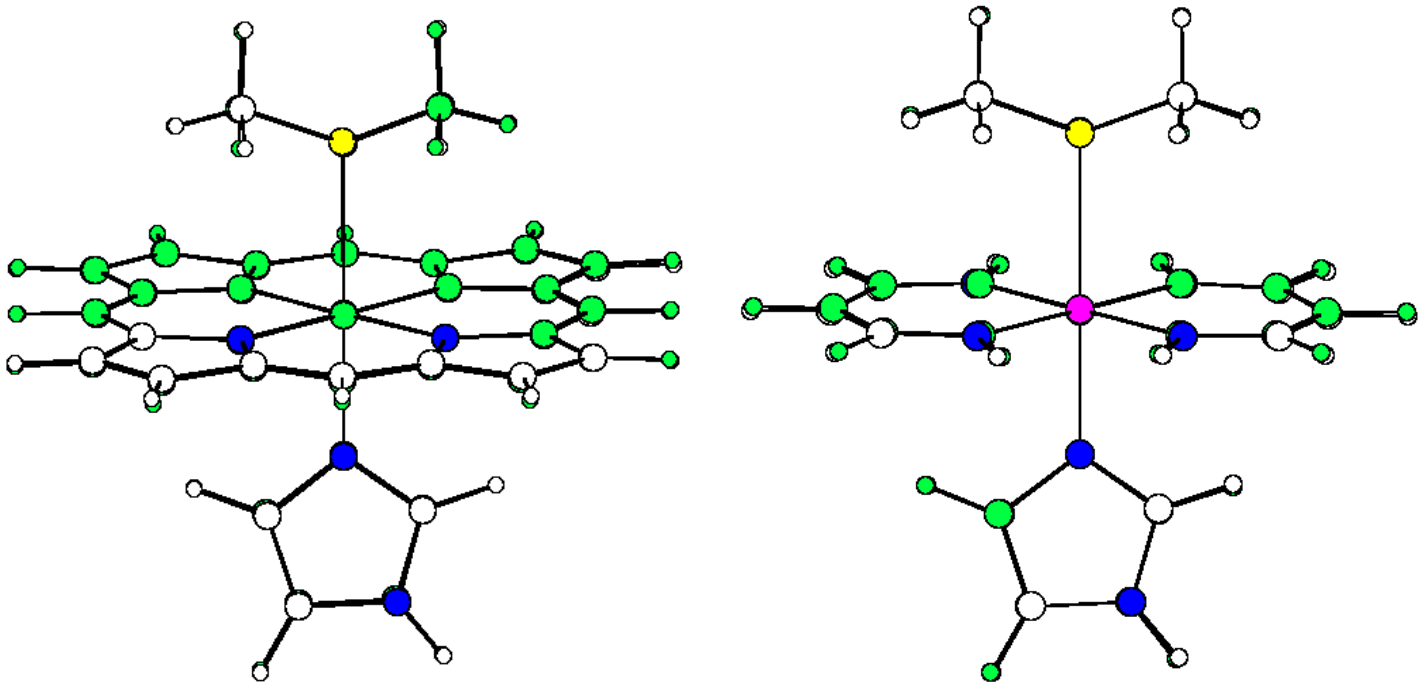

Figure 7. The difference in geometry between the reduced and oxidised (shaded) forms of Fe(porphine)(imidazole)-($S(CH_3)_2$) (left) and $Fe(NH(CH)_3NH)_2$(imidazole)($S(CH_3)_2$) with a broken porphyrin ring.

protein complete the octahedral coordination sphere of the iron ion. They are typically histidine or methionine, although other groups are occasionally encountered [92]. The iron ion alternates between Fe(II) and Fe(III) during electron transfer, always in the low-spin state.

Porphyrin is an interesting group. In its metal-free form it is free of strain and very stable [70]. However, as it is a cyclic molecule formed by covalent bond and with the ring system constrained by aromaticity, the central hole has a quite fixed size, appropriate for ions with a radius of 60–70 pm [70]. This means that low-spin Fe(II) (ionic radius 61 pm) should fit well into the hole, whereas low-spin Fe(III) should be slightly too small (ionic radius 55 pm). Thus, we would expect the porphyrin ring to elongate the Fe(III)–N_{Por} bonds, making them more similar to Fe(II)–N_{Por} bonds. Thereby the inner-sphere reorganisation energy would be reduced and the rate of electron transfer increased.

We have tested this suggestion by calculating the inner-sphere reorganisation energy of iron porphine (a haem group without the peripheral substituents) and of $Fe(NH(CH)_3NH)_2$ (c.f. Figure 7). In the latter model, the porphyrin ring has been split into two halves and the pyrole rings have been removed. Therefore, the molecule can no longer exert any ring strain in this molecule, but it retains the double negative charge, the number of carbon bonds in each half-ring, and almost the same ligand properties. Thus, differences in the reorganisation energy should reflect primarily strain in the porphyrin ring. For the axial ligands, we used in both cases imidazole and $S(CH_3)_2$ as models of histidine and methionine, respectively.

The results of these calculations are shown in Table 2. They show that the porphyrin ring elongates the Fe–N_{Por} distances in both oxidation states, but more for Fe(III) (9 pm) than for Fe(II) (~3 pm). Therefore, the small model gives rise to appreciably larger changes in the equatorial Fe–N_{Por} distances upon reduction (5–6 pm) than the porphyrin model (1 pm). The changes for the axial ligands are similar to those of the full porphyrin model (smaller for Fe–N_{His} but larger for Fe–S_{Met}). Consequently, the reorganisation energy of the small model is twice as high as the one of the porphyrin model, 16 compared to 8 kJ/mole. Thus, covalent strain decreases the reorganisation energy for the haem group in the cytochromes by 8 kJ/mole. Naturally, this increases the rate of electron transfer for the cytochromes.

This example shows that covalent strain can be of a functional value. However, the strain is found in a macrocyclic cofactor and not in a protein. Considering our harmonic models, this is not unexpected. To constrain metal bonds, we need something with a larger force constant. Thus, we need covalent bonds and they must be parts of a ring system in order to avoid that changes in angles and torsions relax the strain.

We also note that the observed strain energy is not very large, only 8 kJ/mole. This is a typical result – we seldom see distortion energies larger than this in native proteins and cofactors. In fact, Liljefors and coworkers have argued that a molecule is distorted by less than 12 kJ/mole when bound to a protein [58]. Nature is

Table 2. Geometries and inner-sphere reorganisation energies (kJ/mole) for two cytochrome models, calculated in the low-spin state.

Model	Oxidation state	Reorganisation energy	Distance to Fe (pm)		
			N_{Por}	N_{His}	S_{Met}
$Fe(porphine)(Im)(S(CH_3)_2)$	II	4.2	202	203	243
	III	4.1	201	200	244
$Fe(NH(CH)_3NH)_2(Im)(S(CH_3)_2)$	II	7.3	198–199	202	244
	III	8.3	193	202	247

not wasteful with binding energies (12 kJ/mole corresponds to an increase in the dissociation constant by a factor of 120) [5].

Protein or model strain?

Our final example is perhaps the most interesting, because it compares directly a metal site in a protein with an inorganic complex designed to mimic it. Such synthetic analogues [93] are widely used in bioinorganic chemistry and they are supposed to be the best way to study how the protein modifies the chemical properties of a metal sites. In fact, it is widely assumed that inorganic models are flexible and strainfree [13].

Let us consider the Cu_A site in cytochrome *c* oxidase and nitrous oxide reductase [94–97]. It is essentially a dimeric blue copper site with two copper ions bridged by two cysteine ligands (Figure 8). Each copper ion has an additional histidine ligand and a weakly bound axial ligand, either a methionine sulphur or a backbone carbonyl oxygen. Cu_A is also an electron carrier, alternating between the fully reduced and the mixed-valence (Cu^I + Cu^{II}) states. In the latter state, the single unpaired electron is delocalised between the two copper ions.

An inorganic model of the mixed-valence Cu_A site has been synthesised by Tolman and coworkers [98] (Figure 9a). It differs from the Cu_A site in the proteins in some conspicuous ways, as can be seen in Table 3. In particular, the Cu–Cu distance is longer and the bonds to the axial ligands are shorter in the inorganic model. It has been shown by a combination of experimental and theoretical techniques that this difference can be traced down to a difference in the electronic ground state of the two complexes: In the protein, the singly occupied orbital is σ^* antibonding with respect to the Cu–Cu axis, whereas it is π bonding in the inorganic model complex [99,100].

It has been suggested that the natural, unstrained state of Cu_A is the one found in the inorganic model, and that the short bond in the protein can be attributed to protein strain [101]. More precisely, it has been suggested that the protein enforces long Cu–S_{Met} and Cu–O distances onto the site (the distances to the axial ligands in the model are very short, 212 pm).

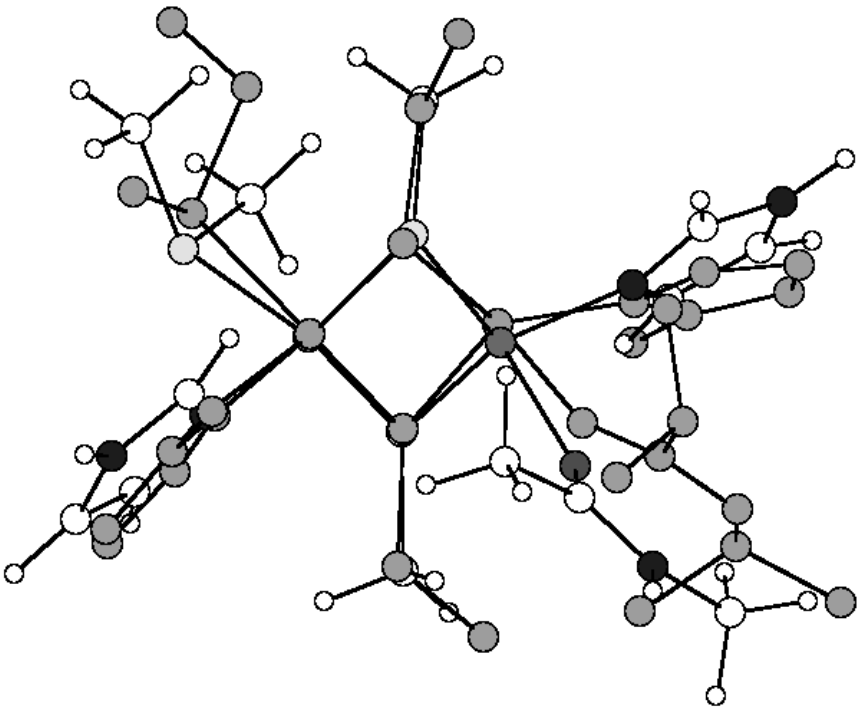

Figure 8. The optimised structure of the σ^* mixed-valence (Im)($S(CH_3)_2$)Cu(SCH_3)Cu(Im)($CH_3CONHCH_3$) complex compared to the crystal structure of the Cu_A site in cytochrome *c* oxidase (shaded) [104].

Table 3. Geometry and stability (in kJ/mole) of some optimised structures with relation to Cu_A and the mixed-valence model complex synthesised by Tolman and coworkers [98]. The Cu_A model is $(Im)(S(CH_3)_2)Cu(SCH_3)Cu(Im)(CH_3CONHCH_3)$ [28].

Complex	State	Cu–Cu	Cu–S_{Cys}	Cu–N	Cu–S_{Met}	Cu–O	S–Cu–S	Relative Energy
Cu_A model	I+I	257	233–247	207–211	240	250	117	
Protein; X-ray [102]	I+I	247	226–231	198–207	247	260	108–113	
Protein; EXAFS [103]	I+I	251–252	231–238	195–197			115	
Cu_A model	I+II π	310	227–236	203–210	242	219	95–97	0.0
Cu_A model	I+II σ^*	248	231–235	202–209	245	220	114–116	1.2
Protein, X-ray [100,104–108]	I+II σ^*	220–258	217–240	185–211	239–272	219–277	111–119	
Protein, EXAFS [103, 109]	I+II σ^*	243–246	229–233	195–203			115	
Model complex [98]	I+II π	290–293	223–230	209–213			100	
$Cu_2S_2N_4C_{22}H_{46}^+$	I+II π	304	228–237	217–221			99	0.0
$Cu_2S_2N_4C_{22}H_{46}^+$, constrained	I+II π	258[a]	229–232	221–227			112	17.5
$((NH_3)_2Cu(SCH_3))_2^+$	I+II π	309	230–233	215–217			96	0.0
$((NH_3)_2Cu(SCH_3))_2^+$	I+II σ^*	248	233	215			115	1.6

[a] This bond length was kept fixed during the geometry optimisation

The reduced charge donation to the copper ions should then be compensated by shortening the other copper–ligand distances, including the Cu–Cu distance. This would lead to formation of a Cu–Cu bond and the change in the electronic ground state, and it has been suggested to significantly alter the reduction potential of the site in the protein.

We have studied the Cu_A site with the same methods as the blue copper proteins [28] and found no evidence of any significant covalent strain. The optimum vacuum structure of both the reduced and mixed-valence (σ^*) states are imposingly similar to the structure found in the protein (Figure 8 and Table 3). We could also obtain the π state as a stable structure, and it is energetically almost degenerate with the σ^* state. The Cu–Cu, Cu–S_{Met}, and Cu–O interactions are extremely flexible and can alter the reduction potential by at most 100 mV (the reduction potential of the model complex is 530 mV lower than for Cu_A in the protein). In particular, a change in the electronic ground state can be expected to change the reduction potential by no more than 10 mV. Similarly, we have found no evidence that covalent strain would significantly influence the inner-sphere reorganisation energy of the protein site.

Therefore, we investigated instead the model complex. As can be seen in Figure 9a, it uses quite poor models for the histidine and axial ligands, viz. amine groups for all four ligands. Moreover, all the ligand atoms are connected by covalent links. We optimised the structure of the full model complex using the same methods as for the Cu_A models. The result is shown in Figure 9b and Table 3. It can be seen that the crystal structure is reasonably well reproduced; the general structure of the two complexes is very similar, but the calculated Cu–Cu, Cu–S, and Cu–N distances are slightly too long.

The optimised structure is also quite similar to the π structure of the Cu_A model. However, the Cu–N distances are 7–15 pm longer in the Tolman model than in the Cu_A model, showing that amine groups are appreciably weaker ligands than imidazole. The amine group seems to be a reasonable model for the carbonyl ligand in Cu_A, because both bind at a distance of ~220 pm, whereas it is a poor model of the methionine ligand, binding more than 20 pm too close. This shows that the difference in the bonds to the axial ligands is mainly caused by the poor ligand models used in the Tolman complex.

Furthermore, the ligands in the Tolman

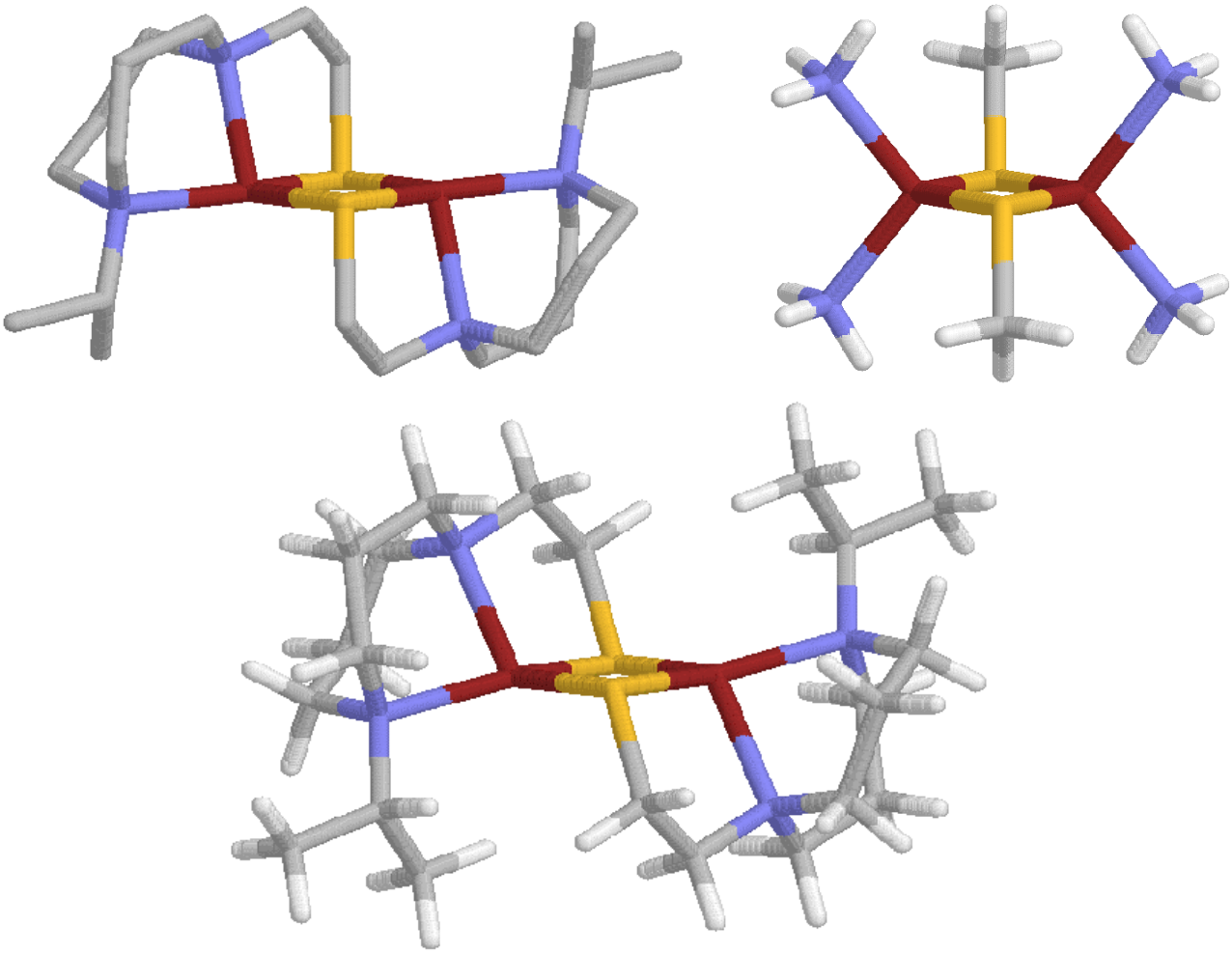

Figure 9. The crystal structure of the mixed-valence complex prepared by Tolman and coworkers [98] (a; upper left) and two optimised models of it: (b, lower) $Cu_2S_2N_4C_{22}H_{46}^+$ in the π state and (c, upper right) $((NH_3)_2Cu(SCH_3))_2^+$ in the σ* state.

model strongly stabilise the π electronic state. We have not been able to find a stable structure with a short Cu–Cu and a σ* electronic state for the model complex. At a Cu–Cu distance of 258 pm (the optimum distance for our Cu_A model plus the difference between the optimum Cu–Cu bond length in the Tolman complex and the calculation), the structure is destabilised by 18 kJ/mole.

In order to estimate the effect of strain in the macrocyclic connections between the ligands in the model, we optimised a small model without these links, $((NH_3)_2Cu(SCH_3))_2^+$ (Figure 9c). As can be seen in Table 3, the π state of this model is quite similar to the full model, with similar bond lengths and angles around the copper ions. However, for this small model, a stable σ* state could also be found, with an optimum Cu–Cu distance of 248 pm (Figure 9c). Most interestingly, this state is practically degenerate with the π state (as in the Cu_A model).

Thus, the destabilisation of the σ* state in the full model complex is caused by the connections between the ligands. From Figure 9c, it can be seen that in the stable σ* states, the four amine groups are placed symmetrically above and below the CuS_2Cu plane. There, they interact with one lobe of the singly occupied Cu 3*d* orbital, thereby stabilising the complex. However, in the full model complex, the macrocyclic connections force two amine groups almost into the CuS_2Cu plane, whereas the other two are far from the plane. This strongly favour the π structure, where the amine groups in the CuS_2Cu plane can overlap with the singly occupied Cu 3*d* orbital, whereas the other two show a very small overlap.

This shows that the difference between the

protein and the model complex actually is caused by strain. However, not strain in the protein but in the model. Again, we see that covalent bonds in a ring are necessary to introduce significant strain in a metal complex. Yet, the most important conclusion is that results obtained with model complexes should not be accepted without considering whether it is a realistic model of the protein site. In particular, inorganic models are not necessarily strainless.

CONCLUDING REMARKS

In this review we have addressed the importance of strain for the function and properties of various metal protein. We have emphasised the importance of defining what you mean by strain (What is the reference state? What interactions are included in the concept? What is the functional value of the strain? What is significant strain?). If we do not use the same definition of strain, endless discussion may arise around a non-existing discrepancy. Moreover, we have pointed out that strain should be discussed quantitatively in energy terms, because chemical transformations are determined by energy differences. It should also be recognised that any metal necessarily becomes slightly distorted when bound to a protein and that both the metal and the protein are normally distorted. Since metal–ligand bonds typically are stronger than the interactions that determine the local orientation of protein ligands (dihedral angles and Van der Waals interactions), the protein typically distort more than the metal [4–6]. In order to introduce significant covalent strain in a metal site, cyclic ligands are often necessary. Thus, we have seen significant strain in the porphyrin ring and in a macrocyclic model complex. However, we have in no case found any indication of a functional role for covalent strain in the proteins we have examined.

Acknowledgements

This investigation has been supported by grants from the Swedish Natural Science Research Council, and by the European Commission through the TMR program. It has also been supported by computer resources of the Swedish Council for Planning and Coordination of Research, Parallelldatorcentrum at the Royal Institute of Technology, Stockholm, the National Supercomputer Centre at the University of Linköping, the High Performance Computing Centre North at the University of Umeå, and Lunarc at Lund University.

REFERENCES

1. Haldane, J. B. S. (1930) Enzymes, Longmans, Green & Co., p. 182.
2. Pauling, L. (1948) Am. Scient. 36, 51.
3. Stryer, L. (1995) Biochemistry, 5th ed., Freeman & Co., New York, pp. 188, 218–222, 339.
4. Warshel, A. (1991) Computer modelling of chemical reactions in enzymes and solutions, J. Wiley & Sons, New York, pp. 209–211.
5. Levitt, M. (1974) Peptides, polypeptides and proteins, (Blout, E. R., Bovey, F. A., Goodman, M., Lotan, N. eds.), pp. 99–102, Wiley, New York
6. Fersht, A. (1985) Enzyme Structure and Mechanisms, pp. 341–342, W. H. Freeman & Co., New York.

7a. Marzilli, L. G., Toscano, J., Randaccio, L., Bresciani-Pahor, N. & Calliaris, M. (1979) J. Am. Chem. Soc. 101, 6754.

7b. Padmakumar, R., Padmakumar, R. & Banerjee, R. (1997) Biochemistry, 36, 3713.

8a. Ghosh, P., Shabat, D., Kumar, K., Sinha, S. C., Grynszpan, F., Li, J., Noodleman, L. & Keinan, E. (1996) Nature, 382, 339–341.

8b. Poulos, T. L. (1996) J. Biol. Inorg. Chem. 1, 356–359.

8c. Archer, M., Carvalho, A. L., Teixeira, S., Moura, I., Moura, J. J. G., Rusnak, F. & Romão, M. J. (1999) Prot. Sci. 8, 1536.

9a. Collman, J. P., Brauman, J. I., Halber, T. R. & Suslick, K. S. (1976) Proc. Natl. Acad. Sci USA, 73, 3333–3337.

9b. Kachalova, G. S., Popov, A. N. & Bartunik, H. D. (1999) Science, 284, 473–476.

10. Vallee, B. L. & Williams, R. J. P. (1968) Proc. Nat. Acad. Sci. USA 59, 498–505.
11. Williams, R. J. P. (1995) Eur. J. Biochem. 234, 363–381
12. Gray, H. B. & Malmström, B. G. (1983) Comm. Inorg. Chem. 2, 203–209.
13. Malmström, B. G. (1994) Eur. J. Biochem. 223, 711–718.
14. Lumry, R. & Eyring, H. (1954) J. Phys. Chem. 58, 110–120.
15. Comba, P. (1999) Coord. Chem. Rev. 182, 343.

16. Malmström, B. G. (1965) Oxidases and related redox systems (King, T. E., Mason, H. S., Morrison, M. eds), Wiley, New York, vol. 1, pp. 207–216.
17. Ryde, U., Olsson, M. H. M., Roos, B. O. & Pierloot, K. (1996) J. Mol. Biol. 261, 586–596 .
18. De Kerplel, J. O. A. &, Ryde, U. (1998) Prot. Struct., Funct., Genet., 36, 157–74.
19. De Kerpel, J. O. A., Pierloot, K., Ryde, U. & Roos, B. O. (1998) J. Phys. Chem. B 102, 4638–4647.
20. Ryde, U. & Olsson, M. H. M. (2001) Geometry, strain, and reorganisation energies of blue copper models in the protein Inten. J. Quant. Chem., in press.
21. Olsson, M. H. M., Ryde, U., Roos, B. O. (1998) Prot. Sci. 7, 2659–2668.
22. Olsson, M. H. M. & Ryde, U. (1999) J. Biol. Inorg. Chem., 4, 654–663.
23. Ryde, U. (1995) Protein Science 4, 1124–1132.
24. Ryde, U. (1996) Eur. J. Biophys. 24, 213–221.
25. Ryde, U. (1996) J. Comp.-Aided Mol. Design. 10, 153–164.
26. Ryde, U. & Hemmingsen, L. (1997) J. Biol. Inorg. Chem. 2, 567–579.
27. Ryde, U., Olsson, M. H. M., Roos, B. O., De Kerpel, J. O. A. & Pierloot, K. (2000) J. Biol. Inorg. Chem., 5, 565–574.
28. Olsson M. H. M. & Ryde U. (2000) Quantum chemical calculations of the Cu_A site in cytochrome *c* oxidase, submitted to J. Am. Chem. Soc.
29. Sigfridsson, E., Olsson, M. H. M. & Ryde, U. (2001) Inner-sphere reorganisation energy of iron-sulphur clusters studied by theoretical methods, Inorg. Chem., in press.
30. Sigfridsson, E., Olsson, M. H. M. & Ryde, U. (2001) A comparison of the inner-sphere reorganisation energies of cytochromes, iron–sulphur clusters, and blue copper proteins., J. Phys. Chem., B. submitted.
31. Pierloot, K., De Kerpel, J. O. A., Ryde, U., & Roos, B. O. (1997) J. Am. Chem. Soc. 119, 218–226.
32. Siegbahn, P. E. M. (2001) Modeling aspects of mechanisms for reations catalyzed by metalloenzymes, J. Am. Chem. Soc., submitted.
33. Gray, H. B., Malmström, B. G. & Williams, R. J. P. (2000) J. Biol. Inorg. Chem. 5, 551–559.
34. Zhou, H.-X. (1997) J. Biol. Inorg. Chem., 2, 109–113.
35. Hertwig, R.H. & Koch, W. (1997) Chem. Phys. Lett. 268, 345.
36. Bauschlicher, C.W. (1995) Chem. Phys. Lett. 246, 40.
37. Siegbahn, P. E. M. & Bolmberg, M. R. A. (1999) Annu. Rev. Phys. Chem. 50, 221–249.
38. Siegbahn, P. E. M. & Bolmberg, M. R. A. (2000) Chem. Rev. 100, 421–437.
39. Hehre, W. J., Radom, L., Schleyer, P. v. R. & Pople, J. A. (1986) Ab initio molecular orbital theory, Wiley-Interscience, New York.
40. Ryde, U., Olsson, M. H. M., Borin Carlos, A. & Roos, B. O. (2001) The dependence of the geometry of blue copper protein models on the, method, basis sets, and model size. Theor. Chem. Acc., in press.
41. Andersson, K., Malmqvist, P.–Å. & Roos, B. O. (1992) J. Chem. Phys. 96, 1218.
42. Pople, J. A., Head-Gordon, M. & Raghavachari, K. (1987) J. Chem. Phys. 87, 5968.
43. Curtiss, L. A., Raghavachari, K., Trucks, G. W. & Pople, J. A. (1991) J. Chem. Phys. 94, 7221.
44. Møller, C. & Plesset, M. S. (1934) Phys. Rev. 46, 618.
45. Sharp, K.A. (1990) Annu. Rev. Biophys. Biophys. Chem. 19 301.
46. Honig, B. (1995) Science, 268, 1144.
47. Gunner, M.R. & Honig, B. (1991) Proc. Natl. Acad. Sci. USA 88 9151.
48. Zhang, L. Y. & Friesner, R. A. (1995) J. Phys. Chem. 99, 16479–16482.
49. Wu, J. H. & Reynolds, C. A (1996) J. Am. Chem. Soc. 118, 10545–10550.
50. Swartz, P.D., Beck, B.W. & Ichiye, T. (1996) Biophys. J. 71, 2958.
51. Li, J., Fisher, C. L., Konecny, R., Bashford, D. & Noodleman, L. (1999) Inorg. Chem. 38, 929–939.
52. Stephens, P. J. Jollie, D. R. & Warshel, A. (1996) Chem. Rev. 96 2491.
53. Pierloot, K., De Kerpel, J. O. A., Ryde, U., Olsson, M. H. M. & Roos, B. O. (1998) J. Am. Chem. Soc. 120, 13156–13166.
54. Bajorath, J. Li, Z., Fitzgerald, G., Kitson, D. K. Farnum, M. Fine, R. M., Kraut, J. & Hagler, A. T. (1991) Proteins, Struct. Funct. Genet. 11, 263–270.
55. Lee, F. S., Chu, Z. T. & Warshel, A. (1993) J. Comput. Chem. 14, 161–185.
56. Frenkel, D. & Smith, B. (1996) Understanding molecular simulations, Academica Press.
57. Jensen, F. (1999) Introduction to Computational Chemistry, John Wiley & Sons Lth, Chichester.
58. Boström J., Norrby P.-O. & Liljefors T. (1998) J. Comp.-Aided Mol. Design 12, 383–396.
59. Singh, U. C. & Kollman, P. A. (1986) J. Comp., Chem. 7, 718.
60. Svensson, M., Humbel, S., Froese, R. D. J.,

Matsubara, T., Sieber, S., Morokuma, K. (1996) J. Phys. Chem. 100, 19357.
61. Eurenius, K. P., Chatfield, D. C., Brooks, B. R. (1996) Int. J. Quant. Chem. 60 1189.
62. Field, M. L. (1998) in The encyclypaedia of computational chemistry, P. v. R. Schleyer, N. L. Allinger, T. Clark, J. Gasteiger, P. A. Kollman, H. F. Schaefer III & P. R. Schreiner (eds.), John Wiley & Sons, Chichester, p. 2255.
63. Ryde, U., Nilsson, K. & Lecerof, D. (2001) Quantum chemical geometry optimisations in proteins using crystallographic raw data, J. Comput. Chem., submitted.
64. Cornell, W. D., Cieplak, P., Bayly, C. I., Gould, I. R., Merz, K. M., Ferguson, D.M., Spellmeyer, D. C., Fox, T., Caldwell, J. W. & Kollman, P. A., (1995) J. Am. Chem. Soc. 117, 5179–5197.
65. Williams, R. J. P. (1963) Molecular basis of enzyme action and inhibition (Desnuelle, P. A. E. ed.), Pergamon Press, Oxford, pp. 133–149.
66. Guckert, J. A., Lowery, M. D., Solomon, E. I. (1995) J. Am. Chem. Soc. 117, 2817–2844.
67. Randall, D. W., Gamelin, D. R., LaCroix, L. B. & Solomon, E. I. (2000) J. Biol. Inorg. Chem. 5, 16–29.
68. Guss, J. M., Bartunik, H. D., Freeman, H. C. (1992) Acta. Cryst. B48, 790–807.
69. Williams, R. P. J. (1985) J. Mol. Catal. 30, 1–26.
70. Kaim, W. & Schwederski, B. (1996) Bioinorganic chemistry: inorganic elements in the chemistry of life, John Wiley & Sons, Chichester, pp. 22–27.
71. Sykes, A. G. (1990) Adv. Inorg. Chem. 36, 377–408.
72. Adman, T. (1991) Adv. Prot. Chem. 42, 145–197.
73. Messerschmidt, A. (1998) Struct. Bond. 90, 37–68.
74. Cotton, F. A. & Wilkinson, G., (1988) Advanced inorganic chemistry, Wiley, New York.
75. Shepard, W. E. B., Anderson, B. F., Lewandoski, D. A., Norris, G. E. & Baker, E. N. (1990) J. Am. Chem. Soc. 112, 7817–7819.
76. Marcus, R. A. & Sutin, N. (1985) Biochim. Biophys. Acta, 811, 265–322.
77. Larsson, S. (2000) J. Biol. Inorg. Chem., 5, 560–564.
78. Wittung–Stafshede, P., Hill, M. G., Gomez, E., Di Bilio, A. J., Karlsson, B. G., Leckner, J., Winkler, J. G., Gray, H. B. & Malmström, B. G. (1998) J. Biol. Inorg. Chem. 3, 367–370.
79. Malmström, B. G. & Leckner, J. (1998) Curr. Opin. Chem. Biol. 2, 286–292.
80. Olsson, M. H. M., Ryde, U., Roos, B. O. & Pierloot, K. (1998) J. Biol. Inorg. Chem. 3, 109–125.
81. Farver, O., Jeuken, L. J. C., Canters, G. W. & Pecht, I. (2000) Eur. J. Biochem. 267, 3123–3129.
82. Nar, H., Messerschmidt, A., Huber, R., Van der Kamp, M. & Canters, G. W. (1992) FEBS Lett. 306, 119–124.
83. Kitajima, N. (1992) Adv. Inorg. Chem., 39, 1–77.
84. Mandal, S., Das, G., Singh, R., Shukla, R., Bharadwaj, P. K. (1997) Coord. Chem. Rev. 160, 191–235.
85. Hellinga, H. W. (1998) J. Am. Chem. Soc. 120, 10055–10066.
86. Botuyan, M. V., Toy-Palmer, A., Chung, J., Beroza, P., Case, D. A. & Dyson, H. J. (1996) J. Mol. Biol. 263, 752–767.
87. Libeu, C. A. P., Kukimoto, M., Nishiyama, M., Hornouchi, S. & Adman, E. T. (1997) Biochemistry 36, 13160–13179.
88. Pascher, T., Karlström, G., Nordling, M., Malmström, B. G. & Vänngård, T. (1993) Eur. J. Biochem. 212, 289–296.
89. Palmer, G. & Reedijk, J. (1991) Eur. J. Biochem. 200, 599.
90. Cowan, J. A. (1997) Inorganic biochemistry, an introduction, Wiley-VCH, New York.
91. Lane, R. W., Ibers, J. A., Rankel, R. B., Papaefthymiou, G. C. & Holm, R. H. (1975) J. Am. Chem. Soc. 99, 84.
92. Fraústo da Silvia, J. J. R. & Williams, R. P. J. (1994) The biological chemistry of the elements, Clarendon Press, Oxford.
93. Holm, R. H. 1977 Acc. Chem. Res. 10, 427–434.
94. Babcock, G. T. & Wikström, M. (1992) Nature, 356, 301.
95. Malmström, B. G. & Aasa, R. (1993) Eur. J. Biochem., 325, 49.
96. Beinert, H. (1997) Eur. J. Biochem., 245, 521.
97. Kroneck, H., Antholine, W. E., Kastrau, D. H. W., Buse, G., Steffens, G. C. M. & Zumft, W. G. (1990) FEBS Lett., 268, 274.
98. Houser, R. P., Young, V. G. & Tolman, W. B. (1996) J. Am. Chem. Soc., 118, 2101–2102.
99. Williams, K. R., Gamelin, D. R., LaCroix, L. B., Houser, R. P., Tolman, W. B., Mulder, T. C., DeVries, S., Hedman, B., Hodgson, K. O. & Solomon, E. I. (1997) J. Am. Chem. Soc., 119, 11501–11514.
100. Farrar, J. A., Neese, F., Lappalainen, P., Kroneck, P. M. H., Saraste, M., Zumft, W. G. & Thomson, A. J. (1996) J. Am. Chem. Soc. 118, 11501–11514.
101. Gamelin, D. R., Randall, D. W., Hay, M. T., Houser, R. P., Mulder, T. C., Canters, G. W., de Vries, S., Tolman, W. B., Lu, Y. & Solomon, E. I.

(1998) J. Am. Chem. Soc. 120, 5246–5263.
102. Brown, K., Tegoni, M., Prudencio, M., Pereira, A. S., Besson, S., Moura, J. J., Moura, I., Cambillau, C. (2000) Nature, Struct. Biol., 7, 191–195.
103. Blackburn, N. J., DeVries, S., Barr, M. E., Houser, R. P., Tolman, W. B., Sanders, D. & Fee, J. A. (1997) J. Am. Chem. Soc., 119, 6135–6143.
104. Yoshikawa, S., Shinzawa-Itoh, K., Nakashima, R., Yaono, R., Yamashita, E., Inoue, N., Yao, M., Fei, M. J., Libeu, C. P., Mizushima, T., Yamaguchi, H., Tomizaki, T. & Tsukihara, T. (1998) Science, 280, 1723.
105. Iwata, S., Ostermeier, C., Ludwig, B. & Michel, H. (1995) Nature, 376, 660.
106. Wilmanns, M., Lappalainen, P., Kelly, M., Sauer-Erisson, E. & Saraste, M. (1995) Proc. Nat. Acad. Sci., 92, 11955.
107. Tusihara, T., Aoyama, H., Yamashita, E., Tomizaki, T., Yamaguchi, H., Shinwawa-Ithoh, K., Nakashima, R., Yaono, R. & Yoshikawa, S. (1995) Science, 269, 1069.
108. Williams, P. A., Blackburn, N. J., Sanders, D., Bellamy, H., Stura, E. A., Fee, J. A. & McRee, D. A., Nature (1999) Struct. Biol., 6, 509–516.
109. Henkel, G., Müller, A., Weissgräber, S., Buse, G., Soulimane, T., Steffens, G. C. M. & Nolting, H.-F. (1995) Angew. Chem. Int. Ed., 34, 1489–1492.
110. Sigfridsson, E. & Ryde, U. (1999) J. Biol. Inorg. Chem., 4, 99–110.
111. Springer, B. A., Egeberg, K. D., Sligar, S. G., Rohlfs, R. J., Mathews, A. J. & Olson, J. S. (1989) J. Biol. Chem. 264, 3057–3060.
112. Olson, J. S. & Phillips, G. N. Jr. (1997) J. Biol. Inorg. Chem. 2, 544–552.
113. Jensen, K. P. & Ryde, U. (2001) Density functional studies of corrins lend no support to a mechano-chemical trigger mechanism, J. Biol. Inorg. Chem., submitted.